Understanding the regulation of human Topoisomerase 1 (TOP1) dynamics and devising TOP1-directed therapeutic strategies

TOP1-DNA covalent complexes (TOP1ccs) are transient DNA-protein adducts arising from TOP1-mediated relaxation of DNA supercoils during replication and transcription. Pathological or drug-induced stabilization of TOP1ccs result in accumulation of lethal (replication and transcription-associated) DNA double strand breaks. Multiple cellular mechanisms (*viz.*, TOP1 phosphorylation, Poly-ADP-ribosylation, SUMOylation, ubiquitination and NEDDylation) efficiently sense TOP1ccs and swiftly degrade or remove the same. Cancer cells are hyper-dependent on TOP1, making it an attractive target of anticancer therapy. Multiple TOP1-targeting drugs (Topotecan, Irinotecan etc.) are in clinical use against ovarian, cervical, lung and pancreatic cancers. TOP1cc removal/degradation factors confer resistance to such drugs. The foregoing work revolves around (a) discovery of CHK1 kinase as a regulator of TOP1 catalysis, and (b) the development of a dual inhibitor of TOP1 and poly-ADP-ribose polymerase (PARP) for efficient targeting of cancer cells.

In order to discover novel TOP1 regulators, we screened 25 small molecule kinase inhibitors (targeting ~42 cellular kinases) for their potential to alter cellular TOP1cc levels. Our results revealed the master checkpoint kinase CHK1 as a positive hit. We validated the finding through biochemical and Fluorescence Recovery After Photobleaching (FRAP) assays. We established the intracellular interaction between CHK1 and TOP1 (through Proximity Ligation and co-immunoprecipitation assays), and demonstrated that CHK1 phosphorylates TOP1 in vitro. Tandem mass spectrometric analysis of catalytically engaged TOP1 from cells revealed that Serine 320, one of the (*in silico*) predicted CHK1 target sites on TOP1 is phosphorylated inside cells. A phospho-resistant mutant of TOP1 (TOP1S320A) revealed that genetic ablation of CHK1-mediated TOP1 phosphorylation results in constitutive stabilization of TOP1S320A on the genome. This was accompanied by copious induction of replication and transcription-associated DNA damage, stabilization of RNA-DNA hybrids (R-loops) and large-scale chromosomal abnormalities. These, and multiple other observations established a previously unreported role of CHK1 in suppression of genomic instability through regulation of TOP1 catalytic activity inside cells. Hence, our study revealed a novel pathway of CHK1-mediated maintenance of genomic stability through regulation of TOP1 (Fig. 1, Left panel).

Owing to the pivotal role of poly-(ADP-Ribose) polymerases (PARPs) in cellular resistance to TOP1 inhibitors, combinatorial inhibition of PARPs and TOP1 inhibitors has been tested in multiple clinical trials. However, pharmacokinetic incompatibilities and dose-limiting toxicities have resulted in mixed outcomes. In order to circumvent such issues, we envisaged the development of a single molecule dual inhibitor of TOP1 and PARP, which would facilitate temporally coupled inhibition of both enzymes. We developed 11 candidate inhibitors involving active pharmacophores derived from Olaparib (an FDA approved PARP inhibitor) and 1,8-naphthalimide (an investigational TOP1 inhibitor). One candidate, DiPT-4, showed significantly higher cytotoxic potential compared to both Olaparib as well as 1,8-naphthalimide. DiPT-4 poisons TOP1 and inhibits PARP activity in vitro. Further, DiPT-4 not only stabilizes TOP1ccs inside cells, but inhibits PARP activation in response to same. Consequently, unlike classical TOP1 poisons, DiPT-4 induces long-lived TOP1ccs without significant degradation of cellular TOP1. Finally, theoretical calculations revealed that DiPT-4 satisfies the majority of criteria for druggability. Our study provided a proof-of-concept for the development of dual inhibitors of TOP1 and PARP1 with significant clinical potential (Fig. 1, Right panel).

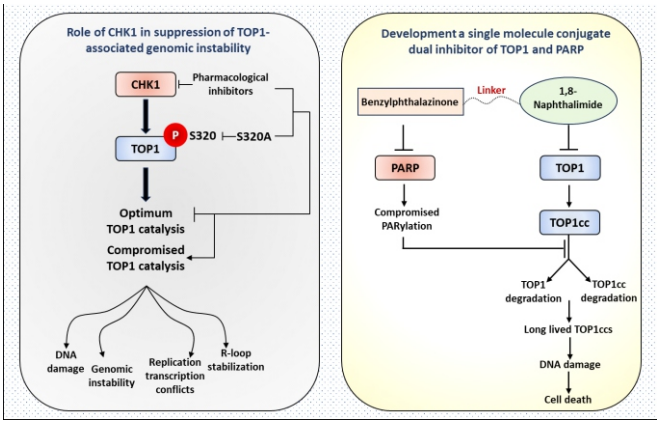

Fig.1: Left panel: A distinct role of CHK1 in prevention of stabilization of TOP1-DNA covalent complex and genomic instability. Right panel: Development of dual inhibitor of Top1 and PARP1 for effective killing of cancer cells.

Taken together, our work reveals novel post-translational regulation of TOP1, and how TOP1 post-translational modifications can be targeted for efficient anticancer therapy.

Highlights of the work being carried out by Ananda Guha Majumdar under the supervision of Dr. Mahesh Subramanian (Guide) and Dr. Birija Sankar Patro (Co-guide) as a part of his doctoral thesis work. This work will be submitted for Ph.D. degree (Life Sciences) to Homi Bhabha National Institute in 2025.

Premature Chromosome Condensation based rapid biodosimetry strategies for high doses and non-uniform exposures

Radiation biodosimetry is an essential part of regulatory investigations, triage and medical management of radiation overexposures. Chromosomal aberration assessed in peripheral blood lymphocytes (PBL) are classical and gold standard biodosimetry markers. To assess the aberrations, PBLs which are usually at resting phase must be stimulated and brought to metaphase for distinct visualization under microscope. Dose estimation takes around 3-5 days for and may require counting up to1000 metaphases. Further, high dose exposures lead to poor metaphase yield due to cell cycle arrest, interphase or mitotic death of heavily aberrated cells. Hence, metaphases may not be available for dose assessment. Challenge further grows when the exposures are localized to a part of the body leading to dilution of cells from un-exposed cells in the blood and resulting in underestimated doses.

Under this thesis, G_0-PCC where mitotic cell fusion to PBLs is used to induced chromosome condensation allowing microscopic visualization at resting phase itself was proposed as alternative, and extensively researched for high dose exposures. With this technique, rapid biodosimetry within 4-6 hours post blood collection can be carried out using quick counting of fragments after Giemsa staining (G_0-PCC-Fragments). It is suitable for high dose and partial body exposure dosimetry as well. In the study, a refined SOP for G_0-PCC was developed, multi-faceted applications were showcased, calibration curve were established to extrapolate dose estimates from an unknown sample. Most importantly, a novel methodology was formulated to distinguish partial exposures from whole body exposures and to derive accurate dose estimations. The technique was refined for the use of cryopreserved mitotic cells to avail them instantly for G_0-PCC upon receipt of accidental exposure case. Further, it was combined with fluorescent in-situ hybridization to analyze aberrations more accurately. G_0-PCC-FISH with locus or chromosome specific probes enabled identification of dicentrics (centromere-FISH), chromosome specific breaks/interchanges (whole chromosome painting and multiplex FISH) and within chromosome arrangements like inversions and interstitial deletions (mBAND-FISH) at resting phase stage of the PBLs. Broad range calibration curves (0-15Gy Co-60 Gamma ray) were established for overall fragments and for breaks combined with interchanges using G0-PCC-FISH for chromosome 1, 2 & 4. For the fragments a linear radiation response was found with a slope of 1.09 ± 0.031 fragments/cell Gy^{-1}(R^2=0.999) with

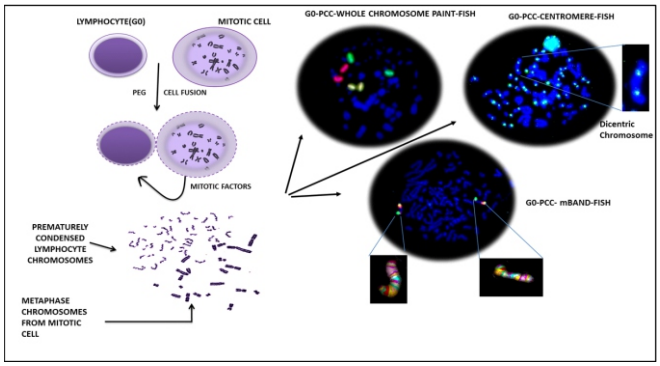

Fig.1: A pictorial diagram of G0-PCC technique and its extensions with FISH (Yadav et.al. Scientific Reports, (2021) 11:13498).

intercept/background of 0.19 ± 0.10 while for G_0-PCC-FISH response followed a linear quadratic curve with $Y=\alpha D+\beta D^2+c$ *where* α= 0.28±0.037 Gy^{-1}, β= 0.039±0.004 Gy^{-2} and c= 0.0568 respectively (R^2= 0.985). The curves were validated with 5 dose blinded samples. Further, no significant difference in the response was observed with respect to age and sex which was evaluated for at 0, 2 & 4 Gy. Further, partial body exposures were simulated ex-vivo with the dilution of exposed blood samples with un-exposed ones. Dilution factors as well as doses were varied among the simulations (8Gy 1:0, 1:1, 1:3 & 1:5 and 4Gy 1:1, 12Gy 1:1). Statistical distribution and dispersion analysis were carried out with three individual donors for all the simulations and compared with that of whole-body exposures. Finally, multiple key features were identified which can distinguish partial exposures from whole body exposures and derive accurate dose estimations. The sensitivity and accuracy of the dose estimates were compared with that of conventional dicentric assay and G_0-PCC-Fragment in all the donors and simulations. It was observed that sensitivity and accuracy of Dicentric assay reduced with increasing dilution and dose but not in PCC methods. G_0-PCC-FISH was found to be most accurate among all.

Highlights of the work carried out by Usha Yadav under the supervision of Dr Nagesh N Bhat as a part of her doctoral thesis work. She was awarded PhD degree from Homi Bhabha National Institute in Life Sciences in 2022.

Studies on Tumor Microenvironment Induced Changes in T Cell Differentiation

Cancer is the unregulated proliferation of transformed cells that can invade nearby tissues. In addition to transformed cells, the tumor microenvironment (TME) includes innate immune cells, adaptive immune cells, fibroblasts, stromal cells, and the extracellular matrix. Cytokines in the TME have an important role in the communication between different cell types, which influences tumor growth and evasion. Transforming growth factor-β (TGF-β) and T regulatory cells (Treg) play a significant role in tumor-induced immunosuppression. Despite the fact that B cells are abundant in tumors, their role in tumor regulation is little understood. Though the involvement of regulatory B cells (Breg) in inflammatory and autoimmune disorders is known, its role in cancer has not been fully investigated.

This thesis investigates Breg's role in Treg differentiation and immunosuppression in cancer as well as the molecular mechanisms of TGF-β-induced Treg generation. We identified that the fibrosarcoma secreted prostaglandin E2 (PGE2), a signaling molecule produced by the breakdown of membrane arachidonic acid by the action of the cyclooxygenase (COX) enzyme, which conferred a Breg like immunosuppressive function in B cells. This tumor-evoked regulatory B cell (tBreg) subtype was found with a unique combination of surface markers along with a TGF-β and IL-10 secretory phenotype not previously reported. Blocking PGE2 synthesis by NS-398, a pharmacological inhibitor of COX2 or PGE2 signaling in B cells with PGE2 receptor antagonists, inhibited the generation of tBregs. The administration of NS-398 to tumor bearing mice markedly reduced tumor burden, lowered Breg and Treg production and rescued T cell responses. These tBregs converted $CD4^+$ T cells to Treg cells, suppressing T cell responses via TGF-β release. SB431542, a small-molecule inhibitor of TGF-β receptor, inhibited TGF-β signaling in T cells, prevented the formation of tBregs, and rescued T cell responses in vitro. The administration of SB431542 to tumor-bearing mice significantly reduced tumor burden and increased T cell responses. To identify inhibitors of Tregs, we screened 160 compounds from an epigenetic inhibitor compound library, as epigenetic pathways are involved in the differentiation of naïve T cells to Tregs. Using an IFN-γ production-based functional screening strategy, we identified two compounds, EPZ004777 and FG-2216, that lowered the expression of Foxp3, the master regulator of Tregs, and its downstream target genes and impaired Treg's suppressive capacity.

Epigenetic modifications are heritable alterations in gene expression that are not attributable to changes in DNA sequences. The precise epigenetic changes involved in TGF-β-induced Treg cells are not fully understood. Using chromatin immunoprecipitation (ChiP) assays, we performed epigenetic profiling of the *Foxp3* locus in Tregs. TGF-β-induced Tregs showed higher levels of H3K4me3, H3K27ac, and lower levels of H3K27me3 and DNA methylation. In Treg generated by physiologically relevant tBregs and PGE2Bregs, higher H3K4me3 and lower H3K27me3 were observed. However, either DNA methylation

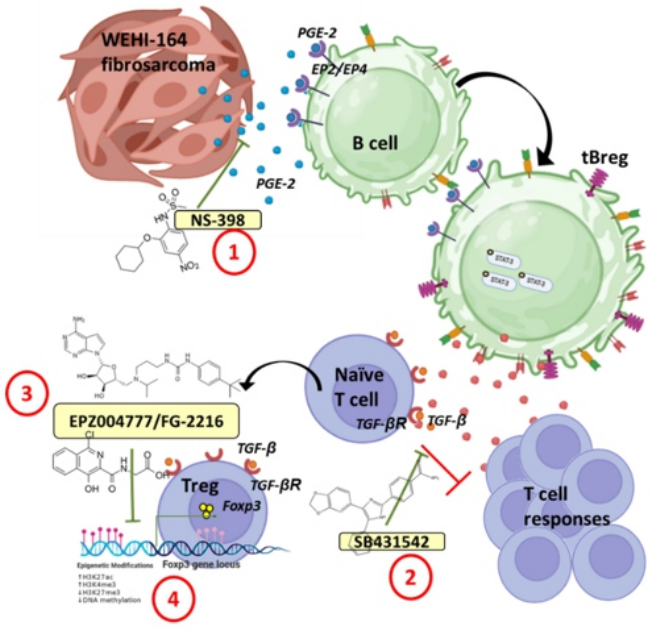

Fig.1: Immunosuppression in the tumor microenvironment: (1) NS-398, a pharmacological inhibitor of COX2; (2) SB431542, a small-molecule inhibitor of TGF-β receptor; (3) EPZ004777 and FG-2216, epigenetic inhibitors of T regulatory cells; (4) Epigenetic landscaping of the Foxp3 locus in T regulatory cells.

was significantly reduced with no change in H3K27ac or H3K27ac was hyperacetylated with no alteration in DNA methylation. Epigenetic profiling of the *Foxp3* locus therefore indicate that increasing H3K4me3 or decreasing H3K27me3 as well as increasing H3K27ac or decreasing DNA methylation are the minimal epigenetic requirements for Foxp3 expression and Treg phenotype.

Many researchers have elucidated the roles of several players in the TME, including dendritic cells, macrophages, NK cells, etc., but the role of B cells and tumor-evoked Bregs has received less attention. The work described in this thesis addresses this critical aspect of the TME and answers several key problems. This is the first-time epigenetic landscaping of TGF-β-induced Tregs has been done to determine the minimum needed modifications. This thesis has also identified two promising epigenetic modifiers as well as COX-2 and TGF-βR inhibitors as potential immunotherapeutics.

Highlights of the work carried out by Kavitha Premkumar under the supervision of Dr. Bhavani S. Shankar (Guide) as a part of her doctoral thesis work. She was awarded a Ph.D. degree from Homi Bhabha National Institute in Life Sciences in 2022.

Studies on Macrophage Conditioned Medium Induced Tunneling Nanotubes and Microplasts Formation in Human Breast Cancer Cells

Tumor-associated macrophages (TAMs) are major infiltrating innate immune cells in the tumor microenvironment (TME) and are associated with poor prognosis in breast cancer patients. The complex milieu of inflammatory cytokines, chemokines, and growth factors secreted by infiltrating macrophages in the TME acts on cancer cells in a paracrine manner and regulates several stages of cancer progression. However, the effect of pro-inflammatory cytokines secreted by macrophages on novel modes of communication via tunneling nanotubes (TNTs) and microplasts in cancer remains elusive. This thesis explores the impact of macrophage-conditioned medium (MΦCM) on breast cancer cells, revealing that MΦCM mimics the inflammatory TME, induces an epithelial-to-mesenchymal transition (EMT) phenotype, and enhances cell migration in MCF-7 cells. Additionally, MΦCM induces TNT formation and stimulates the release of cytoplasmic fragments, referred to as microplasts.

MΦCM-treated MCF-7 cells were found to be viable and migratory, suggesting that microplasts derived from these cells are not apoptotic bodies. Time-lapse microscopy reveals that microplasts exhibit independent migration and also show the dynamic process of microplast release from parent cancer cells through TNT-like structures. In addition, the data also show novel modes of TNT formation facilitated by migratory microplasts, leading to the formation of a complex network of cells. The presence of metalloproteinases in microplasts suggests their role in invasion and metastasis. Furthermore, transcriptomic and proteomic analyses of isolated microplasts reveal their similarity to parent cells in terms of mRNA and protein cargo, potentially serving as carriers of intercellular signalling.

Despite the known roles of TNTs and macrophages in cancer, the impact of macrophage-induced TNTs on therapy resistance remains unclear. Additionally, the mechanisms underlying macrophage-driven TNT and microplast formation are not well understood. In this study, it was shown that TNT formation in MΦCM-treated MCF-7 cells contributed to increased resistance to doxorubicin. Transcriptomic analysis of these treated cells revealed activation of the NF-κB and focal adhesion pathways, along with upregulation of genes involved in epithelial-mesenchymal transition (EMT), extracellular remodeling, and actin cytoskeleton reorganization. By using pharmacological inhibitors targeting key proteins within these pathways, it was demonstrated that TNT and microplast formation in MΦCM-treated MCF-7 cells was mediated by the PKC/Src/NF-κB and p38 signaling pathways. These findings provide valuable insights into the complex mechanisms of intercellular communication in breast cancer, driven by TAMs, and highlight potential therapeutic targets for cancer treatment.

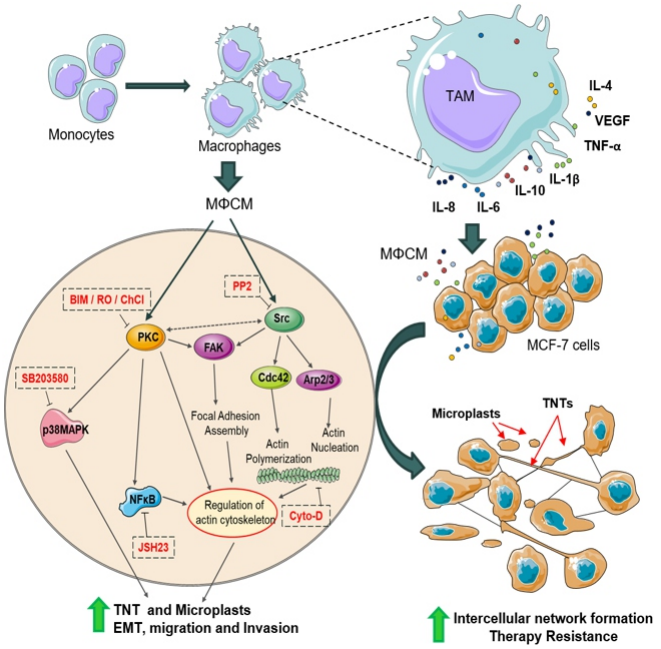

Fig.1: Macrophage conditioned medium (MΦCM) increased epithelial-to-mesenchymal transition (EMT), migration, tunneling nanotube (TNT), and microplast formation in MCF-7 cells via PKC, Src, NF B, and p38 signaling (Melwani et. al, BBA Reviews on Cancer, 2023 and Melwani et. al, Cellular Signaling, 2024).

Highlights of the work carried out by Dr. Pooja Kamal Melwani under the supervision of guide Prof. B. N. Pandey as a part of her doctoral thesis work. She was awarded PhD degree from Homi Bhabha National Institute in Life Sciences in 2023.

Development of Peptides Targeting HER2-Receptor Overexpression in Breast Cancer

Breast cancer has the highest global incidence amongst all the cancer types. Early detection is the key for timely intervention and proper treatment planning. Human epidermal growth factor receptors (HER2) are over-expressed in breast cancers and are associated with poor prognosis and aggressively metastatic disease. The present work focused on development of HER2-targeting ligands for breast cancer detection and therapy. Towards this, peptides exhibiting attractive advantages of high target affinity, specificity, favorable pharmacokinetics, and ease of synthesis were chosen as suitable ligands. A HER2-targeting A9 peptide was subjected to several modifications (pegylation, cyclization, D-amino acid incorporation, retro variant) to overcome the challenges of *in vivo* enzymatic degradation.

The peptides were synthesized by solid phase synthesis methodology manually (Fig. 1), purified and characterized. Peptides were then radiolabeled with theranostic radionuclide, $^{177}LuCl_3$. ^{177}Lu-labeled original A9 peptide exhibited rapid blood clearance resulting in low tumor uptake. It also underwent high metabolic degradation. The pegylated variant, [^{177}Lu]Lu-DOTA-PEG$_4$-A9 demonstrated improved metabolic stability, tumor uptake and retention.

Further the peptide was cyclized on-resin by copper (I)-catalyzed azide-alkyne cycloaddition (CuAAC) 'click reaction'. The cyclic variant [^{177}Lu]Lu-DOTA-c[Tz]-A9 exhibited increased binding affinity towards HER2-positive cells, high metabolic stability and tumor uptake. To introduce changes in the backbone all the L-amino acids were replaced by D-amino acids and thus inverso- and retro-inverso A9 peptides were synthesized. These peptides had enormously enhanced metabolic stability, tumor uptake/retention was observed to be higher for the retro-inverso variant. Another analogue studied was the retro-variant where the C- and N-terminal were swapped and the L-amino acids were arranged in reverse manner. The retro variant showed most promising results with highest tumor uptake amongst the six investigated A9 analogs (Fig. 2). SPECT/CT imaging studies further demonstrated higher *in vivo* tumor retention of the retro analogue (Fig. 3).

In conclusion arrangement of amino acid sequence in reverse manner either D-amino acids (retro-inverso peptide) or L-amino acids (retro peptide) conferred improved features to the A9 peptide. Swapping of C- and N-terminal (retro) introduces significant changes in the backbone of the peptide. In the case of presently studied HER2-targeting A9 peptide, swapping imparted positive features suggesting higher participation of backbone towards receptor interaction.

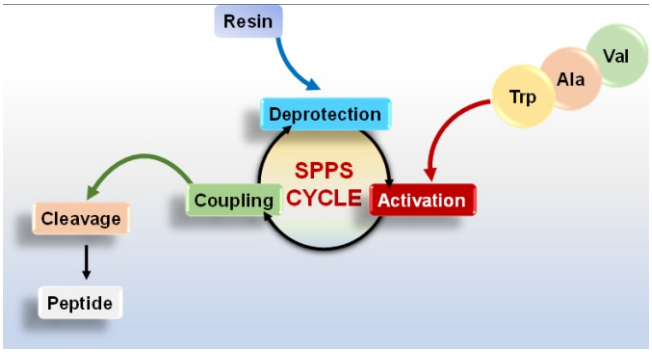

Fig.1:Solid phase peptide synthesis methodology scheme

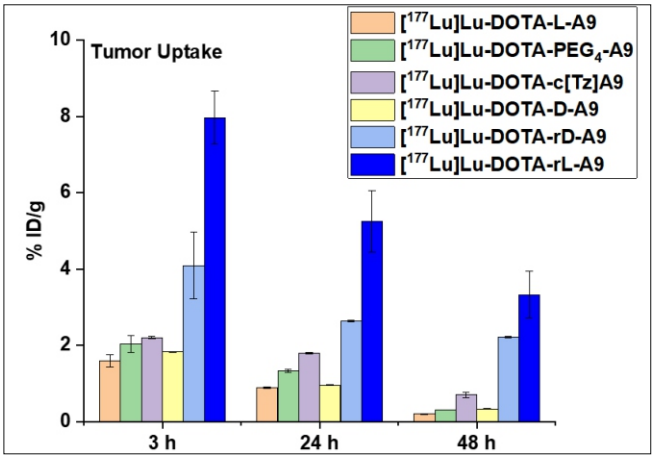

Fig.2: Tumor uptake of A9 peptide analogues.

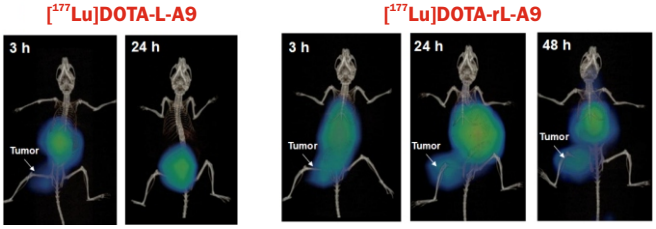

Fig.3: SPECT/CT images of female SCID mice bearing SKBR3 tumor xenografts.

Highlights of the work carried out by Amit Kumar Sharma under the supervision of Dr. Drishty Satpati (Guide) and Dr. Tapas Das (Co-guide) as a part of his doctoral thesis work. He was awarded PhD degree from Homi Bhabha National Institute in Chemical Sciences in 2024.

Mechanistic Studies on Ubiquicidin-Membrane Interaction & Development of Infection Imaging Probes

The work presented in this thesis encompasses research aimed at comprehending the interaction mechanism between the antimicrobial peptide Ubiquicidin (UBI) and bacterial membranes. Subsequently, infection imaging probes were developed for detecting bacterial infections like osteomyelitis and fever of unknown origin, which pose challenges for conventional detection techniques.

Significantly, this thesis marks the first report providing a mechanistic understanding of the antimicrobial action of ribosomal protein S30/Ubiquicidin (UBI). Using phospholipid membrane models, various biophysical studies i.e., Dynamic Light Scattering (DLS), Circular Dichroism (CD), Infrared Spectroscopy (IR), and Quasielastic Neutron Scattering (QENS) were conducted to unravel the intricacies of UBI-membrane interactions. Additionally, microbiological investigations were carried out to grasp the impact of UBI on bacterial growth and survival. Overall, these findings revealed that UBI selectively binds to bacterial membranes, inducing a conformational change in this peptide. This interaction exerts a catastrophic effect on the bacterial membrane by altering its fluidity, causing permeabilization, and inducing depolarization, ultimately leading to the loss of bacterial viability. Furthermore, it was demonstrated that UBI fragments, i.e., UBI (29-41) and UBI(31-38), also retained their binding and selectivity towards bacteria. Importantly, UBI and its derivatives were shown to be non-toxic to human cells, through haemolysis and cell toxicity studies.

Leveraging the mechanistic insights gained through biophysical and microbiological methods, efforts were made to develop UBI-derived peptide fragments into infection imaging radiotracers for SPECT (Single Photon Emission Computed Tomography) and PET (Positron Emission Tomography) imaging to detect S. *aureus*-driven focal infections. UBI fragments, namely UBI (29-41) and UBI (31-38), were labeled with ^{99m}Tc and ^{68}Ga for this purpose, and the resulting radiotracers underwent *in vitro* and *in vivo* studies. UBI-derived radiotracers were confirmed to be selective towards bacteria through *in vitro* uptake in bacterial cells and *in situ* detection of S. *aureus* in animal models of infection and sterile inflammation. Furthermore, efforts were also made to enhance the detection sensitivity and salt tolerance of UBI-based radiotracers by modifying UBI (29-41). The introduction of the Lysyl-phosphatidyl-glycerol (Lys-PG) specific group, 2-APBA, at the C-terminal of UBI (29-41) resulted in an improved infection imaging probe, which interacted synergistically via electrostatic and covalent modification of Lysyl-PG via iminoboronate with the bacterial membrane. Through this work, the conjugation of 2-APBA is demonstrated as an effective strategy for improving the therapeutic potential of existing antimicrobial peptides (AMPs). Remarkably, this work also resulted in the successful clinical translation of ^{68}Ga-labeled UBI fragments as a PET-based radiotracer for the early identification of bacterial focal infections. The formulated radiotracers were evaluated at KMCH, Coimbatore, PGI, Chandigarh, and MPMMRC, Varanasi, and could detect lung infection, soft tissue infection, bone prosthesis, and spinal TB (tuberculosis) infections with high sensitivity (Fig. 1).

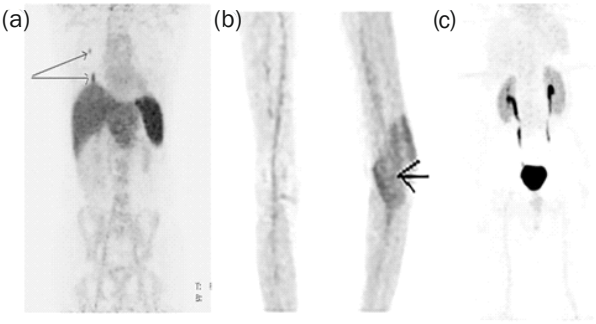

Fig.1: PET/CT images of patients injected with ^{68}Ga-UBI (31–38) at 1 h p.i. (a) lung infection (true positive scan). (b) soft tissue infection in left knee (true positive scan) joint. (c)Image of a suspected left hip prosthesis infection (true negative scan).

Highlights of the work carried out by Jyotsna Bhatt under the supervision of Dr. Archana Mukherjee (Guide) and Dr. Mukesh Kumar (Co-guide) as a part of her doctoral thesis work. She was awarded Ph.D degree from Homi Bhabha National Institute in Life Sciences in 2023.

Interplay Between DNA Damage Repair, Replication Stress and Autophagy Under the Functional Deficiency of PARP in Cancers

Small molecule inhibitors of Poly (ADP-ribose) polymerases (PARPi) are approved for clinical usage in patients with hereditary breast and ovarian cancers with compromised homologous recombination (HR) mediated DNA repair, a strategy referred to as synthetic lethality (Fig. 1A). However, therapeutic resistance remains a challenge, with only about ~50% of the target cohort of patients (*viz*. 5-15% of the total breast and ovarian cancer patients that harbour BRCA1/2 mutations, or are HR deficient) responding well to this therapy (Fig. 1B).

Recent findings indicate that HR-proficient cancers can also be targeted with the combination of PARP inhibitors and chemosensitizing agents. This necessitates research into avenues targeting cancers with PARP inhibitors along with targeting alternative pathways in HR-proficient cancers. Moreover, why certain HR-proficient cancers are *de novo* PARPi resistant, while certain others are comparatively sensitive was envisaged in this thesis. Understanding these mechanisms enable extension of PARPi therapy to a wider set of patients with BRCA1/2-wild-type (WT) or HR-proficient cancers.

Autophagy, a cellular process aiding in the removal of dysfunctional and superfluous biomolecules and organelles, is implicated in acquired chemoresistance and is recognized for its interplay with DNA damage repair pathways. However, molecular underpinnings of this interplay, and how and if this could be exploited for cancer therapy, is unclear. In this work, we successfully demonstrated that autophagy confers *de novo* resistance to PARP inhibitors in HR-proficient breast cancers. Using chloroquine, an anti-malarial drug now repurposed as an autophagy inhibitor, we show that combined PARP and autophagy inhibition leads to better therapeutic outcome in breast cancer cells and in SCID mice xenograft models. Mechanistically, DNA repair switched from faithful HR pathway to deleterious 53BP1-mediated NHEJ which further led to genomic instability and mitotic catastrophe under this autophagy- and PARP inhibited condition (Fig. 1B,C). Additionally, we showed synergistic induction of cancer cell death both *in vitro* and *in vivo*, when resveratrol, natural molecule, was combined with PARPi, talazoparib. This synergistic action of the combination was attributed to the inhibition of late-stage autophagy and suppression pro-survival pathways such as PI3K leading to p38 mediated apoptosis and mitotic catastrophe (Fig. 1B,C).

DNA replication is a vulnerability in many cancers and replication stress induction presents as an attractive therapeutic strategy that can be harnessed for efficient cancer therapy. PARP inhibitors induce replication stress mainly by trapping PARPs on DNA forming PARP-DNA-PARPi ternary complexes, and dysregulating replication fork speed. Resveratrol analogues are also reported to enhance replication stress. In this regards, we have shown the combinatorial therapies involving talazoparib with resveratrol analogue, 4,4'-dihydroxystilbene (DHS), post screening a library of resveratrol analogues for DNA damage induction and HR downregulation. Talazoparib (PARPi) *plus* DHS was found to induce extensive DNA damage double strand breaks, and downregulate RAD51, a key modulator of both DNA repair and replication, to induce extensive replication stress and S-phase catastrophe (Fig. 1D). This suggests a novel replication-dysfunction-mediated approach for enhancing PARPi sensitivity in cancers.

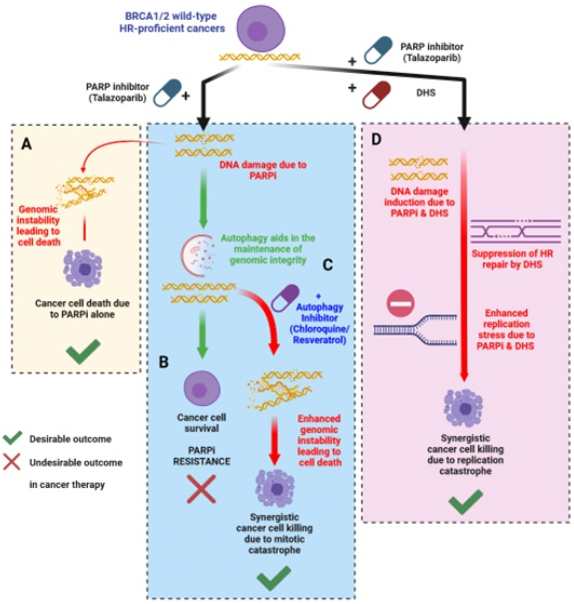

Fig.1: Schematic of the PARP inhibitor combinatorial strategies used to sensitize BRCA1/2 wild-type HR proficient cancers. (A, B, C and D represent different outcomes of PARPi therapy as depicted).

In conclusion, we have identified that the combination therapies involving PARP inhibition with agents that suppress/modulate autophagy such as chloroquine and resveratrol, or those inducing replication stress such as DHS show promise in sensitizing HR-proficient cancers to PARPi induced cell death (Fig. 1A-D). This study unravels the potential for the broadening of the limited scope of PARP inhibitors to a larger population of patients with HR-proficient breast cancers and for tumours resistant to PARP inhibitors.

Highlights of the work carried out by Ganesh Pai B under the supervision of Dr. Birija Sankar Patro (Guide) as a part of his doctoral thesis work. This PhD thesis was submitted recently (May, 2024) to Homi Bhabha National Institute for the PhD Award in Life Sciences.

Advancing Retrospective, Cumulative and Rapid Biodosimetry- Innovative Molecular Cytogenetics Approach

As scientific advancements continue, the utilization of radiation is becoming more prevalent in our daily lives, thus increasing the likelihood of inadvertent exposures. Biodosimetry serves as a crucial tool, providing accurate dose measurements in the absence of physical dosimetry methods or corroborating results obtained through physical dosimetry, particularly in cases of exposures exceeding 100 mGy. This study investigates various biodosimetry methods to address dosimetry challenges across a wide range of radiation exposure scenarios.

Radiation-induced phosphorylation of γH2AX and 53BP1 stands out as reliable, reproducible, and highly sensitive markers for biodosimetry. This study has meticulously characterized the decay kinetics and dose-response curves essential for rapid biodosimetry, offering a valuable resource for dose estimation within 96 hours of exposure during radiological emergencies. Investigation into γH2AX and 53BP1 foci induction, progression, saturation, and decay was conducted using both microscopy and flow cytometry techniques. Notably, a rapid exponential rise in foci induction was followed by an exponential decay over 96 hours for both methods. Data analysis revealed that the initial kinetics followed the function $Y=A - Be^{(-kt)}$ for both techniques. Subsequent to saturation, microscopic foci detection exhibited a bi-exponential decay pattern described by the function $Y= A + Be^{(-k1t)} + Ce^{(-k2t)}$, while flow cytometry followed a single exponential decay pattern represented by $Y= A + Be^{(-kt)}$. It is worth to note here is that the foci formation rate (k) and decay rates (k1 and k2) showed no dependency on the initial doses delivered. The established calibration curves were rigorously validated using three blinded samples with dicentric and Reciprocal-Translocation (RT), with results indicating that the γH2AX assay via microscopy provided the closest estimate at the lowest dose (0.5 Gy, 8% variation), while at higher doses (1 & 2 Gy), all techniques performed almost equally well (maximum 14% variation).

Translocations, considered as stable aberrations, are particularly suitable for dosimetry of cumulative past exposures spanning months to decades. This study focused on analyzing the yield and distribution of translocations (both reciprocal and non-reciprocal), involving painted chromosome pairs 1 and 2, subsequent to *ex vivo* irradiation ranging from 0 to 4 Gy, using blood samples from three volunteers. Approximately 21,000 metaphases were meticulously analyzed, averaging around 7,000 metaphases per individual. All datasets exhibited agreement with the Poisson distribution, facilitating the utilization of Poisson weighted curve fitting. The data were fitted utilizing a linear quadratic model of the form $Y = C + \alpha D + \beta D^2$. The resulting fit yielded a linear coefficient $\alpha = 0.90 \times 10^{-2}$ translocations per cell per Gy and a quadratic coefficient $\beta = 3.58 \times 10^{-2}$ translocations per cell per Gy^2. Given their stability, the Reciprocal-Translocation Dose Response Curve is suitable for cumulative biodosimetry of both recent and past exposures. Conversely, the Non-Reciprocal-Translocation Dose Response Curve, pertaining to unstable aberrations, is applicable solely for biodosimetry of recent exposures.

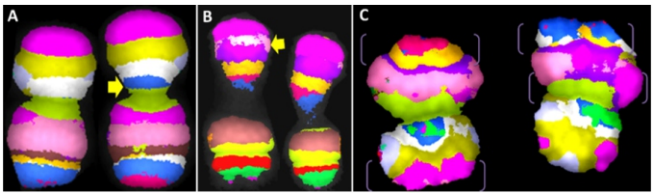

Fig.1: Illustration depicting interstitial deletion of (A) blue and (B) light pink bands from one homolog of the chromosome pair. (C) Represents a complex intrachromosomal rearrangement.

Distinct chromosomal aberrations induced by low and high Linear Energy Transfer (LET) radiations exhibit structural differences. Low LET radiation predominantly induces inter-chromosomal changes, whereas high LET radiation predominantly induces intra-chromosomal rearrangements, which can be visualized and quantified using advanced mBAND-FISH techniques (Fig. 1). Human blood samples were subjected to doses ranging from 0 to 200 mGy of 14 MeV neutrons at the DT neutron facility, Purnima, BARC. Dose Response Curves (DRCs) were generated for interstitial deletions, intra-chromosomal rearrangements, and complex rearrangements, revealing a linear nature with slopes of 2.33, 1.49, and 0.799 aberrations per cell per Gy for interstitial deletions, intra-chromosomal rearrangements, and complex rearrangements, respectively. Interstitial deletions were found to be predominant across all dose points examined. Comparative analysis with low LET radiation (^{60}Co-γ-rays) exposures revealed significantly lower frequencies of intra-chromosomal changes, even at higher doses (0/310 for 2 Gy and 2/352 for 4 Gy).

Utilizing established cytogenetic and immunofluorescence techniques (specifically γH2AX & 53BP1), this study investigated critical clinical cases to assess radiation sensitivity and genetic instability. Genetic instabilities and chromosomal aberrations induced by radiation were analyzed in the lymphocytes of a pediatric Wiscott Aldrich Syndrome (WAS) patient, with a comparison to a healthy volunteer (control). The irradiated WAS sample exhibited a significant excess yield of dicentrics (51%), reciprocal translocations (59.1%), and non-reciprocal translocations (80%) compared to the control sample, indicating a notable increase (ranging from 51% to 80%) in misrepair events. Moreover, analysis of γH2AX foci decay kinetics revealed a sustained elevation in foci numbers up to 48 hours post-irradiation. These results suggest that high radio-sensitivity and genetic instability may predispose WAS patients to cell transformation and genetic complications.

Highlights of the work carried out by Rajesh Kumar Chaurasia under the supervision of Dr. N. N. Bhat (Guide) as a part of his doctoral thesis work. He was awarded a Ph.D. degree from Homi Bhabha National Institute in Life Sciences in 2022.

Detection and Mitigation of Intracellular Labile Iron pool

Iron overload in the human body, whether extracellular (labile plasma iron, LPI) or intracellular (labile iron pool, LIP), generates oxidative stress leading to cell death either via lipid peroxidation and/or DNA damage and is associated with many diseases viz. Heart failure, liver diseases, skin diseases, diabetes, Alzheimer's disease, etc. Hence detection and mitigation of intracellular labile Iron (primarily in Fe^{2+} form due to reductive cellular environment) is important, not only for exploring various iron dependent physiological processes but also for diagnosis and treatment of Iron overload.

Operationally simple, inexpensive, and highly sensitive turn-on fluorescence probes to detect iron overload in living cells are rarely reported. The present studies provided a unique, triplet-stable, Fluorinated Boron-Dipyrromethene (BODIPY) based pro-fluorescent nitroxide (PFN) probe with highly Fe^{2+} selective, high-fold turn-on fluorescence response towards Fe^{2+}. Moreover, the dye detected different amount of intracellular iron in a variety of iron-overloaded cells, which showcased its advantage over other similar probes.

Chelation therapy has emerged as a treatment of choice to mitigate iron overload, and FDA approved chelators e.g. Desferioxamine (DFO) have been the chelator of choice in clinics. However, the drawbacks of DFO towards being cell impermeable and low bio-availability along with short systemic circulation time, have made the use of DFO difficult. In this research, a nanoformulation of DFO was designed, synthesized, characterized, and evaluated in a pre-clinical iron-overload mice model, which demonstrated better iron mitigation along with increased systemic circulation time. These studies will open up the field of nanochelators that can be used as more effective drug candidates for iron overload diseases.

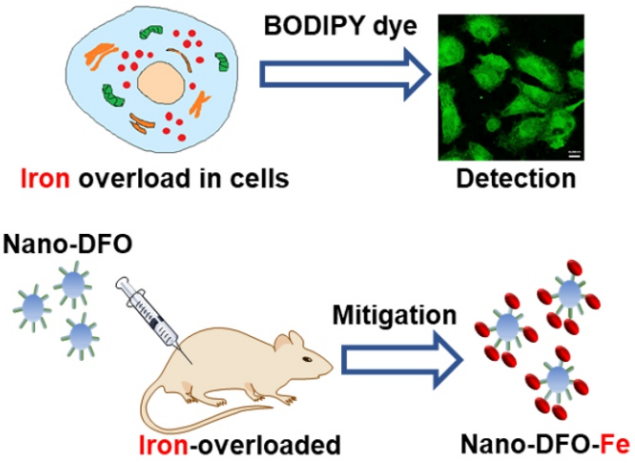

Fig.1: Strategies for detection and mitigation of iron overload.

Highlights of the work carried out by Ms. Pradnya K. Pachpatil under the supervision of Dr. Dibakar Goswami (Guide) as a part of her doctoral thesis work. She will be submitting her thesis in 2025 for a Ph.D. degree from Homi Bhabha National Institute in Life Sciences.

Understanding DNA Repair Pathways to Sensitize Werner (WRN) RECQL Helicase Deficient Cancers

Mutations in WRN protein (DNA helicase) leads to a condition called Werner Syndrome (WS) where patients are predisposed to cancer and premature aging. Cancer patients harbouring tumors with epigenetic inactivation of WRN showed better response to DNA damaging drugs like camptothecin and its derivatives. The present work has explored the novel role of WRN in various compensatory DNA repair pathways and the potential inhibition of these pathways to enhance the efficacy of widely used cancer therapeutic such as radiation and chemotherapy.

We have established that WRN deficient cells are dependent on a critical but compromised CHK1-mediated HR (homologous recombination) pathway for repair of radiation induced DSBs. As, WRN deficient cells (WRN-KD) were found to be hyper sensitive to ionizing radiation in combination with CHK1 inhibitor. Similar to CHK1 inhibitor, WRN-KD cells are also hyper sensitive to radiation in presence of p38 inhibitor. As p38-MAPK activation is regulated negatively by WRN in a CHK1-dependent manner for the repair of IR induced damage. We also showed that CHK1-p38-MAPK axis plays important role in RAD51 mediated HR repair in WRN-deficient cells. Hence, it has been established that inhibiting HR repair pathway either by CHK1 or p38 inhibitor, WRN deficient cells become hyper-sensitive radiation, which can enhance the therapeutic response of radiation treatment of cancer (Fig. 1, left panel).

Our whole genome transcriptome analysis showed a robust activation of NF-KB related gene expression in response to low dose of camptothecin (CPT). CPT, topotecan and irinotecan are used as chemotherapeutics to target Topoisomerase 1 (TOP1) to generate TOP1-covalent complex (TOP1cc) to kill cancer cells. Upon unravelling the detailed molecular mechanism of TOP1-CPT-DNA (TOP1cc) complex formation and removal, we found that WRN is responsible for TOP1cc complex degradation, which leads to activation of NF-KB pathway. Mechanistically, WRN induced TOP1cc complex leads to generation of ssDNA, which phosphorylates CHK1 and later on activate NF-B pathway by increasing nuclear localization of p65. This activation follows the canonical pathway of NF-$_{\kappa}$B activation via ATM and NEMO. Interestingly, neither helicase nor exonuclease activity of WRN was involved in ssDNA generation and NF-KB activation, establishing the non-enzymatic role of WRN in NF-KB activation Fig. 1, middle panel). In preclinical studies, WRN proficient melanoma tumors were highly resistant while WRN-deficient tumors were sensitive to pharmacological treatment of CPT.

Success of cisplatin treatment is limited by its acquired drug resistance and autophagy is one of mechanism responsible for it. In the present study, we revealed that WRN deficient cells are sensitive to cisplatin treatment and increased ROS production, which causes the mitochondrial dysfunction and induce mitophagy. Imperatively, mitophagic clearance and lysosomal fusion with autophagosome were severely impaired in WRN deficient cells. The key adaptor protein p62 was accumulated more while lipidation of LC3 were defective in these cells, suggesting that autophagosome formation is impaired due to lack of LC3 lipidation. ATG7, a key regulator of LC3 lipidation, was significantly downregulated in WRN deficient cells, which further substantiate the defective mitophagy process in these cells. Mechanistically, our in-depth analysis showed that WRN regulates ATG7 expression via resolving several DNA G4-quadruplex structures in the ATG7 gene and assisting maturation of ATG7 mRNA. Together, our study revealed hitherto an unknown function of WRN in mitophagy and its regulation through ATG7 expression (Fig. 1, right panel).

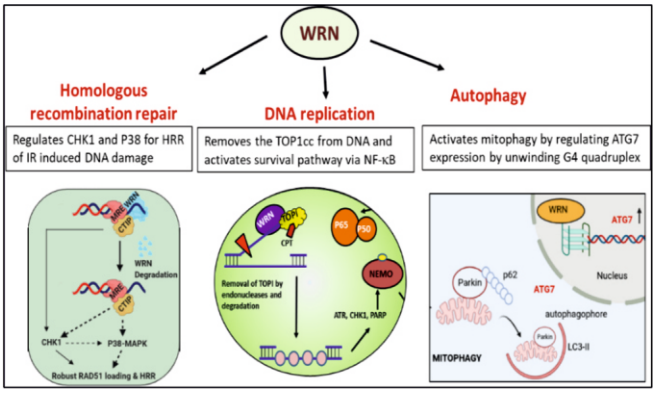

Fig.1: Schematic of the role of WRN in HR repair, DNA replication and NF-kB pathway activation and autophagy by ATG7 gene regulation.

In summary, this investigation highlights important role of WRN in regulating multiple genes like CHK1, p38, p65 localisation and ATG7, which contributes in cell survival pathways such as homologous recombination, NF-B pathway and mitophagy (as shown in Fig. 1). Inhibiting WRN in combination with cancer therapy can lead to better outcome in terms of cancer treatment.

Highlights of the above work was carried out by Pooja Gupta under the supervision of Dr. Birija Sankar Patro (Guide) as a part of her doctoral thesis work. She was awarded Ph. D degree from Homi Bhabha National Institute in Life Sciences in 2022.

Studies on Development of Radioimmunotherapy Agents and Understanding their Mechanism of Action

Breast, ovarian, and gastric cancers often exhibit overexpression of Human epidermal growth factor receptor 2 (HER2), leading to aggressive forms with poor prognoses. Immunotherapy using monoclonal antibodies against HER2, Trastuzumab and Pertuzumab has revolutionized treatment of HER2 positive cancer. However, the emergence of resistance poses a significant challenge, emphasizing the urgency to explore alternative therapeutic approaches. Radioimmunotherapy (RIT) utilizing radiolabeled antibodies has gained significant attention in cancer management, however an ideal radioimmunotherapeutic agent for solid cancers is still not available.

The work documented in the thesis encompasses the development of ^{177}Lu labeled Pertuzumab as RIT agent for targeting HER2 overexpressing cancers. Procedure optimization for conjugating chelators to antibodies,radiolabeling with therapeutic radioisotope Lu-177, characterization by chromatography studies followed by comprehensive biological evaluation in tumor cell lines and animal tumor model was performed. Multiple batches of patient dose of ^{177}Lu labeled Pertuzumab were prepared to verify the reproducibility of results. SPECT imaging studies indicated enhanced tumor uptake and significant retention of the radioimmunoformulation when studied up to 120 h *p.i* confirming its potential as a promising radioimmunotherapy (RIT) agent. Additionally, the radioformulation exhibited a robust tumor-inhibiting response in HER2 tumor-bearing SCID mice. In addition, studies with ^{177}Lu labeled F(ab')$_2$-fragments were performed to compare the difference in the pharmacokinetics of the radioformulations.

Understanding the molecular mechanisms responsible for the clinical synergy observed during combination therapy involving Trastuzumab and Pertuzumab is crucial for effectively managing breast and other similar cancers. While computational models have proposed mechanisms for the synergistic effects of Trastuzumab and Pertuzumab, experimental evidence supporting these hypotheses was lacking. To address this gap, experimental analyses were conducted to assess the interactions of radiolabeled antibodies (Pertuzumab/Trastuzumab) in the presence and absence of a second unlabeled antibody. Furthermore, F(ab')$_2$-fragments of both the antibodies were produced and radiolabeled to investigate the role of the Fc region of the monoclonal antibody in these binding interactions. The study revealed that the radioimmunoconjugates preserve the existing binding synergism between Pertuzumab and Trastuzumab to HER2 receptors and significant binding enhancement of radiolabeled Pertuzumab and its fragments was observed in the presence of Trastuzumab in both *in-vitro* and *in-vivo* testing conditions.

The existence and potential impact of radiation-induced biologic bystander effects (RIBBEs) in radionuclide therapy is inadequately understood. The studies on investigating the RIBBEs mediated by Trastuzumab antibody radiolabeled with three therapeutic radioisotopes , ^{90}Y (a pure β^- emitter), ^{177}Lu (a β/γ emitter), and ^{125}I (an auger electron emitter) were performed. Treatment of cells with radiolabeled formulations not only resulted in inhibitory bystander effects in recipient (bystander) cells but also notable toxicity in irradiated cells (both directly irradiated and donor cell groups) was observed. Moreover, elevated levels of reactive oxygen species were observed at higher doses in bystander cells, suggesting their significant contribution in RIBBE. The thesis work led to the development of radiolabeled formulations suitable for clinical translation. Furthermore, these formulations were utilized to investigate mechanisms aimed at enhancing their efficacy for cancer management.

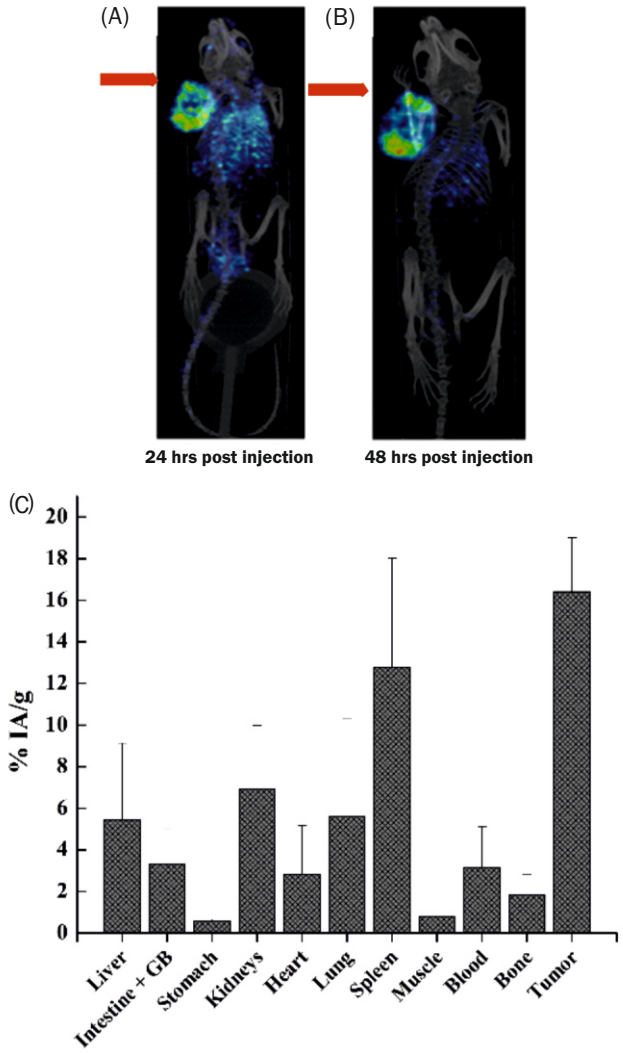

Fig.1: [^{177}Lu]Lu-CHX-A′-DTPA–Pertuzumab injected in SK-OV-3 tumor bearing SCID mice. SPECT/CT imaging studies (A) at 24 h post injection ,(B) 48 h post injection.(C) Biodistribution data showing % Injected activity / gram of tissues at 120h p.i .

Highlights of the work carried out by Dr. Rohit Sharma under the supervision of Dr. Archana Mukherjee (Guide) as a part of his doctoral thesis work. He was awarded Ph.D degree (Life Sciences) from Homi Bhabha National Institute in July 2024.

Development of Targetable Radiolabeled Self-assembly Structures for Combination Cancer Therapychanism of Action

Combination radionuclide therapy (CRT) for cancer treatment involves the use of radionuclide therapy in combination with multiple therapeutic modalities, to target cancer cells through different mechanisms. This approach aims to maximize treatment efficacy while minimizing the development of resistance and reducing the risk of tumor recurrence.

Liposomal formulations have emerged as a powerful tool in cancer management, offering unique advantages in drug delivery and enhancing therapeutic efficacy. These lipid-based nanoformulations can encapsulate a wide range of therapeutic agents, including chemotherapeutic drugs, nucleic acids, and imaging agents, within their aqueous core or lipid bilayer. This encapsulation provides several benefits, such as protecting the payload from degradation, prolonging circulation time, and enabling controlled release at the tumor site. Additionally, surface modifications of liposomes with targeting ligands, such as antibodies or peptides, facilitate active targeting of cancer cells, further enhancing specificity and therapeutic efficacy (Fig. 1)

To leverage these unique strengths of liposomal nanoformulations, work on development of targetable self-assembly structures was undertaken.Liposomes of size < 100 nm were prepared by ethanol injection method. Doxorubicin (Dox), an FDA-approved drug was encapsulated into liposomes using the pH gradient method. These liposomes encapsulating doxorubicin (Lip-Dox) were actively targeted to the HER2 receptor overexpressed in breast cancer using the monoclonal antibody trastuzumab. The conjugation of trastuzumab to Lip-Dox was validated and Ab-Lip-Dox was radiolabeled with ^{99m}Tc and ^{177}Lu using bifunctional chelator conjugated lipid moieties and were characterized using chromatography techniques. The affinity of the Ab-Lip-Dox for HER2 receptor was ascertained by confocal microscopy and cell binding & inhibition studies. The ^{99m}Tc labeled Ab-Lip-Dox showed targeting to HER2 overexpressing SKBR3 xenograft tumor and improved clearance from blood compared to ^{99m}Tc labeled Lip-Dox as observed by SPECT imaging studies (Fig. 2).

Further, ^{177}Lu-labeled Lip-Dox was formulated and evaluated for combinatorial cytotoxicity of Dox and ^{177}Lu at different doses for treatment of breast cancer. The synergistic therapeutic effect was observed at lower doses of Dox (5-50 nM) and ^{177}Lu (1-25 µCi) when used concurrently via radiolabeled Lip-Dox in breast cancer cells. The synergistic effect of Dox and ^{177}Lu was also observed in vivo in SKBR3 tumor bearing animals by tumor growth delay studies. The synergism at lower doses of Dox and ^{177}Lu with non-sphering toxicity will reduce the side effects of the formulations resulting in enhanced therapeutic index.

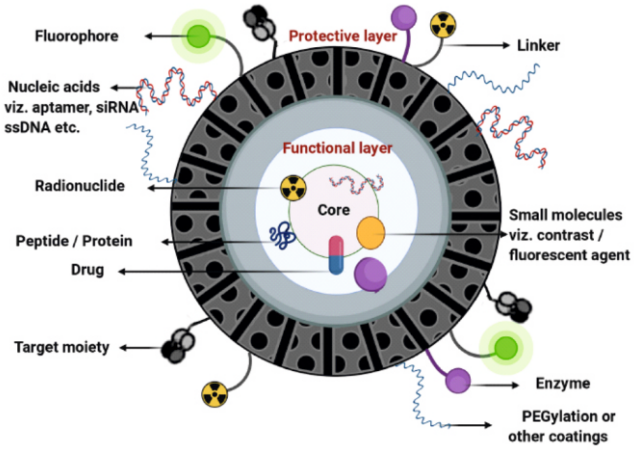

Fig.1: A graphical representation of nanoliposomal formulation that can encapsulate a combination of different anti-cancer therapeutic strategies.

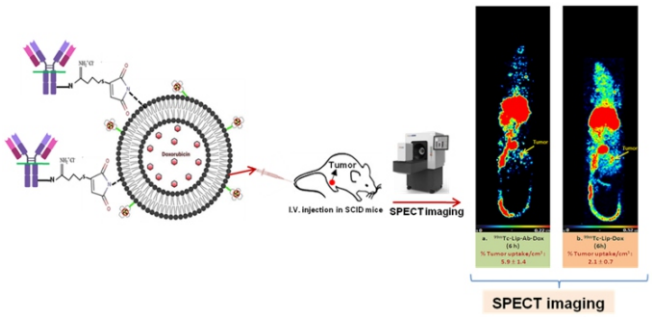

Fig.2: SPECT images after injecting radiolabeled nano formulations in SCID mice bearing SKBR3 tumors.

In this thesis work, radiolabeled nano liposomal formulations loaded with a drug were successfully formulated and were actively targeted to tumors using antibodies for imaging and therapy applications. These formulations hold great promise for personalized cancer treatment through combination radionuclide therapy.

Highlights of the work being carried out by Shishu Kant Suman under the supervision of Dr. Archana Mukherjee (Guide) as a part of his doctoral thesis work. This work will be submitted for Ph.D. degree (Life Sciences) to Homi Bhabha National Institute in 2025.

Exploring the Potential of Novel Radiolabeled Biomolecules and Biomolecule-Drug Conjugates for Imaging and Therapy of Cancers

Nuclear medicine, a specialized field of modern-day medical sciences, uses radiolabeled drugs/biomolecules, known as 'Radiopharmaceuticals', for diagnosis and treatment of various types human ailments. Radiopharmaceuticals play a pivotal role in the management of many diseases, predominantly cancer. As a result, there is a great interest in the development of novel target-specific radiolabeled agents for diagnostic and therapeutic applications. A radiopharmaceutical usually contains a radionuclide and a carrier moiety, which determines the target-specificity of such agents. Therefore, developing radiopharmaceutical requires careful selection of the carrier ligand.

Different carrier moieties, such as, peptides, antibodies, drugs, nano-carriers exhibit preferential uptake in tumorous/cancerous lesions. Porphyrins also exhibit similar tendency to preferentially accumulate in the neoplastic tissues. However, undesired non-target accumulation is one of prime reasons which limit their intended clinical applications. Conjugation of the targeting vectors with suitable secondary targeting moieties may help in circumventing this problem. The work reported in this thesis is related to the development of radiolabeled agents involving porphyrin conjugates and antibody-drug conjugates having unique properties and potential for specifically targeting the tumorous lesions.

Present work involves syntheses of variety porphyrin derivatives and their thorough characterization by standard spectroscopic techniques, such as, UV-Vis, FT-IR, ^{1}H- and ^{13}C-NMR spectroscopy as well as by mass or MALDI-TOF spectrometry. One such porphyrin derivative [5-carboxymethyleneoxyphenyl-10,15,20-tris(4-methoxyphenyl) porphyrin, UTRiMA] was synthesized and radiolabeled with ^{nat}Cu as well as ^{64}Cu with an aim to explore the utility of such complexes in PDT (Photodynamic Therapy) and PET (Positron Emission Tomography), respectively. Detailed biological investigations carried out in healthy as well as cancer cell lines demonstrated significant reduction in photo-cytotoxic potential of porphyrin derivative upon complexation with Cu. However, [^{64}Cu]Cu-UTRiMA exhibited potential as an agent for targeted radionuclide therapy.

In another work, an in-house synthesized porphyrin derivative namely, 5,10,15,20-tetrakis-(4-carboxymethyleneoxyphenyl)porphyrin was conjugated with PAMAM [poly(amidoamine)] dendrimers and subsequently radiolabeled with ^{177}Lu, a well-established therapeutic radionuclide. Biological studies performed with [^{177}Lu]Lu-labeled porphyrin-PAMAM conjugate in tumor bearing small animal models revealed significant accumulation of the radiolabeled particles in the tumor, which was further corroborated through scintigraphic imaging. However, lower retention of the radiolabeled agent in the tumorous lesions at the longer time points may pose a limitation toward its envisaged application as a radio-therapeutic agent.

With an aim to augment the tumor uptake and improve the pharmacokinetic behavior of porphyrin, its conjugation with a cell penetrating peptide (Transactivator of Transcription, TAT) was attempted. Porphyrin-TAT conjugate was synthesized using solid phase synthesis. MTT assay revealed preferential light dependent toxicity for porphyrin derivative which was further enhanced upon peptide conjugation. Fluorescence and flow cytometry studies revealed relatively higher cellular internalization of porphyrin-TAT conjugate in comparison to the porphyrin derivative. Porphyrin-TAT conjugate was further radiolabeled with ^{68}Ga, a generator produced radionuclide used for PET imaging. Ex-vivo evaluation of [^{68}Ga]Ga-porphyrin-TAT complex in fibrosarcoma bearing Swiss mice model revealed higher tumor uptake for [^{68}Ga]Ga-porphyrin-TAT conjugate as compared to [^{68}Ga]Ga-porphyrin. However, observation of higher non-target retention of both the radiolabeled agents during ex-vivo studies might pose limitation towards their possible application in PET imaging.

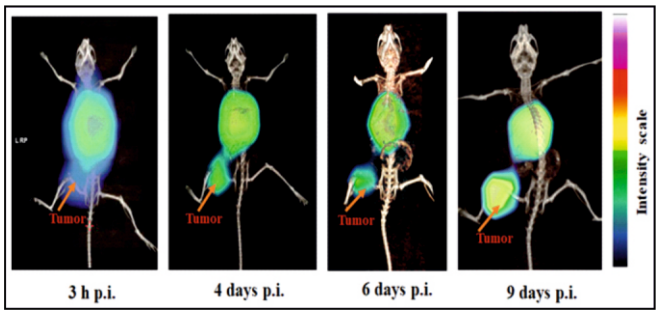

Fig.1: Whole-body SPECT-CT images of the tumor (femur region) bearing Swiss mice acquired after administration of [^{177}Lu] Lu-porphyrin-NLS conjugate at different time-points.

To strike a balance between the hydrophilicity and lipophilicity for obtaining an optimum pharmacokinetic behavior, a porphyrin derivative (UTriMA) was conjugated with NLS sequence [PKKKRKV] (synthesized via solid phase peptide synthesis method). Fluorescence cell imaging studies carried out in HT1080 cancer cells revealed intra-cellular accumulation for the NLS conjugated porphyrin, whereas unconjugated porphyrin failed to reach inside the cells. Porphyrin-NLS conjugate was radiolabeled with ^{177}Lu. Biological distribution studies in fibrosarcoma bearing Swiss mice model revealed significantly higher accumulation and prolonged retention of [^{177}Lu]Lu-porphyrin-NLS conjugate in the tumorous lesion, which was further corroborated by recording serial SPECT-CT images (Fig. 1).

In continuation with the aim of improving the uptake and pharmacokinetic behavior of radiolabeled agents for cancer management, radiolabeled antibody and antibody-drug conjugate were also synthesized during the course of the present work. Conjugation reaction between Rituximab (antibody) and Chlorambucil (drug) was optimized and the resultant antibody-drug conjugate was radiolabeled ^{177}Lu with high radiochemical purity. Ex-vivo studies for the radiolabeled antibody and antibody-drug conjugate, performed in cancer cells and SCID mice bearing Non-Hodgkin's lymphoma xenografts showed significant improvement in the non-target uptake of antibody post-conjugation with the drug (chlorambucil) without compromising the tumor avidity.

Results obtained during above-mentioned studies revealed a definite effect in the targeting ability of molecular cargo upon conjugation with secondary targeting moieties. The studies indicate that this strategy may be helpful in the preparation of radiolabeled biomolecule-drug conjugates to obtain potent radiopharmaceuticals having high tumor uptake and optimum pharmacokinetic behavior for applications in cancer management.

Highlights of the work carried out by Shri Naveen Kumar under the supervision of Prof. Tapas Das (Guide) as a part of his doctoral thesis work. Shri Naveen has submitted his doctoral thesis (in Chemical Sciences discipline) to Homi Bhabha National Institute in April, 2024.

CRISPR Systems and Gene Modulation in Anabaena

Archaea and bacteria possess the 'CRISPR-Cas' systems to combat the invasion of external nucleic acids. CRISPR stands for Clustered Regularly Interspaced Short Palindromic Repeats and refers to the specific genetic sequences found in these organisms. The proteins involved in this defense mechanism are known as CRISPR-associated proteins (Cas proteins). The regions, known as CRISPR loci, present on bacterial genomes, contain repeats as well as short sequences derived from phages or plasmids. Together, Cas proteins and CRISPR loci provide a form of adaptive immunity, defending against external nucleic acid invasions. Cyanobacteria also encode CRISPR systems in their genome. Bioinformatic analysis using various tools and web servers has revealed that *Anabaena* PCC 7120 genome harbors three distinct CRISPR systems: two class 1 systems (type I-D and type III-D) and one class 2 system (type V-K) and a total of eleven CRISPR loci.

In-depth *in silico* analysis of all the proteins related to type I-D locus showed, this system to be the most complete CRISPR system present in *Anabaena* PCC 7120. Genes related to expression, interference module and adaptation components, were identified and found to constitute a complete CRISPR system. 3-D models of all proteins related to the type I-D system were generated using homology modelling/ab initio/threading. Specifically focusing on the type I-D system, we found that the Alr1562 protein played a crucial role, acting as a backbone of the type I-D (CRISPR Associated Complex for Antiviral Defense) CASCADE interference complex. When purified from *E. coli*, Alr1562 exhibited the ability to exist in either a dimeric or higher oligomeric form. Interestingly, Alr1562 showed a stronger binding affinity towards repeat-spacer-repeat (RSR) RNA as compared to a non-specific RNA. The residues essential for RNA binding were identified and subsequently mutated using site-directed mutagenesis. These mutated proteins, mostly existing in dimeric forms, exhibited significantly reduced binding to RNA, demonstrating that dimer formation is independent of RNA binding (Fig. 1A). This marks the first documentation of a Cas7 protein characterization in a photosynthetic organism.

Cyanobacteria, have developed intricate mechanisms to safeguard themselves against oxidative stress caused by increased production of reactive oxygen species (ROS). 2-Cysteine-Peroxiredoxins (2-Cys-Prx), present in all organisms, utilize the two catalytic cysteine residues at their active site to detoxify peroxides. The exogenous CRISPR-dCas9 system from S. pyogenes was employed to generate a knockdown (CRISPR interference, CRISPRi) strain for the Alr4641

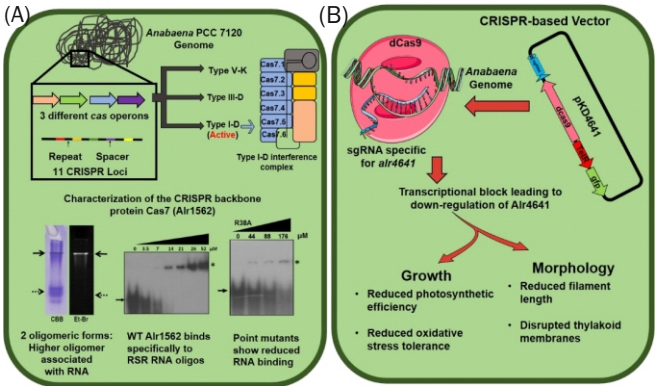

Fig.1: (A) Exploration of endogenous CRISPR system and (B) Use of exogenous CRISPR system to knockdown alr4641 in Anabaena PCC 7120.

protein (Fig. 1B), which is a typical 2-Cys-Prx in *Anabaena* PCC 7120. The growth of An-KD4641 (knockdown strain) was slower with smaller filament size and reduced photosynthetic efficiency as compared to the An-dCas9 (control strain). Ultrastructural analysis (TEM) revealed the knockdown strain to have disrupted and discontinuous thylakoid membranes, whereas the An-dCas9 strain had well-structured, multilayered thylakoid membranes. Interestingly, the total ROS content was higher in An-KD4641 under unstressed conditions. Notably, the knockdown strain was more vulnerable to the oxidative effects of H_2O_2. Furthermore, the knockdown strain exhibited a significantly greater vulnerability to oxidative stress induced by H_2O_2 compared to the control strain.

In conclusion, the work described here has (a) identified the different CRISPR-systems present in Anabaena PCC 7120 (b) thoroughly characterized the Alr1562 protein, identifying the residues responsible for binding to crRNA (c) successfully demonstrated the use of CRISPRi technology in repressing genes in Anabaena, and (d) revealed the vital role of the Alr4641 protein in defending this ecologically significant cyanobacterium against oxidative stress.

Highlights of the work carried out by Prakash Kalwani under the guidance of Dr. Anand Ballal (Guide) and Dr. Devashish Rath (Co-guide) as a part of his doctoral thesis work. He was awarded a Ph.D. degree from Homi Bhabha National Institute in Life Science in 2022.

Understanding the Defence Response to Stem Rust Disease of Wheat

Wheat is one of the important cereals contributing to nutritional security of millions of people worldwide. Wheat production is threatened by stem rust (black rust) disease caused by fungal pathogen *Puccinia graminis* f. sp. *tritici (Pgt)*, which can cause 50–100% loss in yield. In recent years, new pathogenic races of *Pgt* (e.g. Ug99, Digalu race) have emerged overcoming resistance conferred by important *Sr* genes. In the current study resistance response conferred by *Sr24* (major race specific *Sr* gene) was investigated in two wheat Near Isogenic Lines (NILs) using phenotypic, microscopic and transcriptomic analysis. In addition, these responses were also examined in another *Sr* gene (*Sr26*) harbouring genotype. Results showed that, in presence of *Sr24* the resistant NIL showed low infection type (IT) in seedling stage as well as reduced disease coverage at adult plant stage. Time-course study of the disease development showed induction of hypersensitive response (HR)-based resistance within 2–3 days post inoculation (dpi) leading to minute uredia pustule size in the *Sr24* carrier (Fig. 1A). The histological studies showed post haustorial resistance to Pgt with restricted fungal structures at early and late stages (Fig. 1B). Transcriptomics-based analysis showed elevated levels of genes involved in pathogen recognition, multiple signalling pathways involved in activation of transcription factors (TFs) which activate the expression of multiple defence pathways (Fig. 1C). The antifungal responses activated by R gene included elevated ROS levels, synthesis of antifungal secondary metabolites, activation of ion and solute transporters, PR protein induction, cell wall fortification, and modulation of multiple metabolic pathways. Certain antifungal response genes remained upregulated at late stages, showing their sustained involvement in restricting the *Pgt* growth. The DEGs identified in resistant NIL were mapped to the donor genome (*Thinopyrum elongatum*) in vicinity of linked marker to *Sr24* (Fig. 1D). The phenotypic, microscopic and gene-expression study upon Pgt infection in an additional NLR type *Sr* gene (*Sr26*) also showed similar trend, suggesting overlapping resistance mechanism to *Pgt* with some variations (Fig. 1E).

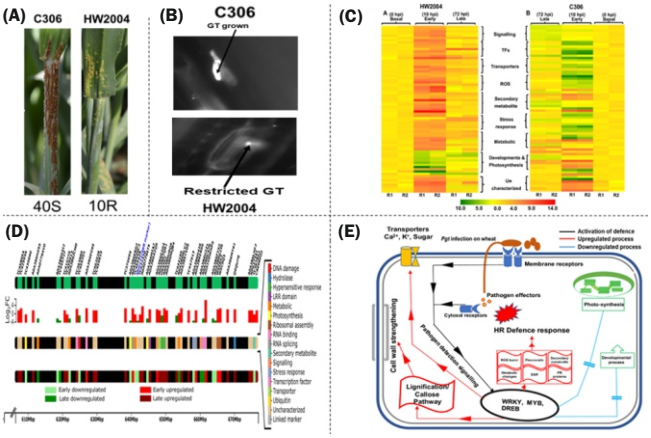

Fig.1: A) Susceptible and resistant response of wheat NILs to Pgt. B) Restriction of Germ Tube (GT) in resistant NIL. C) Expression profile of key genes in NILs upon Pgt infection. D) DEGs mapped on Sr24 donor species genome, in vicinity of linked marker. E) Overall mechanism of resistance to Pgt in wheat.

This research work was carried out by Dr. Gautam Vishwakarma under the supervision of Dr. B. K. Das (Guide) and Dr. Ajay Saini (Co-guide) as a part of his doctoral thesis work. He was awarded a Ph.D. degree from Homi Bhabha National Institute in Life Science in August, 2024.

Forward Genetics of a Chickpea (Cicer Arietinum L.) Mutant Identifies a Novel Locus (CaEl) Contributing to Increased Seed Size, Organ Elongation and Early Vigor

Chickpea is one of the top three grain legumes (pulses) grown worldwide. It is a good source of protein, carbohydrates and dietary fibers. India is the largest producer and consumer of chickpeas and contributes more than 70% (13.54 Mt) of the total world production (18.09 Mt). Chickpea production is challenged by various abiotic and biotic stresses, causing significant yield losses. Trait-based breeding approaches have been useful to counter these challenges. One such trait is 'early vigor', characterized by fast seed germination, seedling growth and early plant establishment with dense canopy. Such a phenotype confers advantages such as reduction of competition from weeds, reduction of direct evaporation, improving plant growth under prevalent stresses etc. Combined with early maturity, plants with high vigor are also suitable for terminal drought prone environments. In the present study, through induced mutagenesis using gamma rays, a novel chickpea mutant was isolated. The mutant showed a distinct phenotype of elongation in vegetative and reproductive organs, than the wild type (WT) (Fig. 1a) and was named "*elongated mutant*" (*elm*). The *elm* also showed early emergence and early vigor that contributed to more shoot biomass at the early vegetative stage. This also resulted in a better performance of elm as compared to the WT in terms of germination and growth under salinity stress. In addition, *elm* accumulated less Na^+ in leaves and a higher proline content indicating a better stress response as compared to WT under salinity stress. The cellular morphology was altered in *elm*. The size of the pavement cells was larger with lesser number of cells per unit area than the WT, indicating that both cell division and cell expansion are affected in *elm* (Fig. 1b). The inheritance study showed monogenic regulation of organ elongation trait with incomplete dominance of WT allele over mutant allele (Fig. 1c). Further, using a 'Bulked segregant analysis' approach, molecular markers linked to this mutation were identified. Genetic mapping study, mapped all markers to single linkage group on chromosome 1 of chickpea genome with one marker (CaGM04793) co-segregated with the mutant locus (*el*) (Fig. 1c). *In-silico* analysis positioned this marker (CaGM04793) in the gene Ca_13541 (LOC101503252 in NCBI database) (Fig. 1d). Polymerase chain reaction to amplify the full-length gene showed a complete deletion of this gene in the mutant (Fig. 1d), with loss of expression in mutant as well as in recombinant inbred lines having mutant phenotype (Fig. 1e). The gene 101503252 showed homology to Arabidopsis AT1G79060, which is annotated as Tetrapeptide Repeat Homeobox Like (TPRXL), with no known function to date. Recently, AT1G79060 was shown to correspond to STIGMA AND STYLE STYLIST 1 in *A. thaliana* regulating

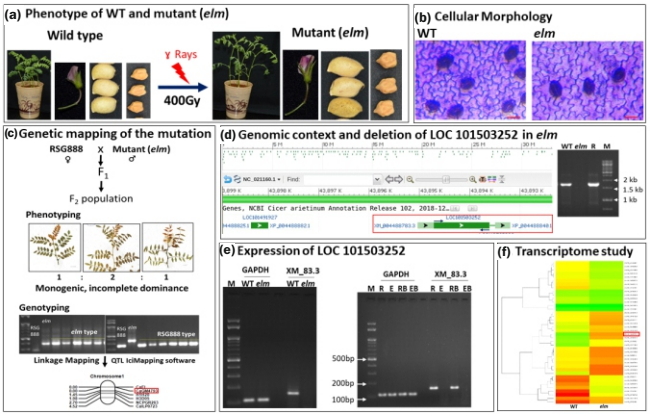

Fig.1: (a) Phenotype of WT and elm (b) Cellular morphology of pavement cells in WT and elm (c) Genetics and mapping of elongation trait (d) Snapshot showing genomic context of gene 101503252 (red box) at NCBI database and PCR amplification showing deletion of gene 101503252 in elm (e). RT-PCR showing loss of CaEl expression in elm (left) and in elm type inbred lines (right), GAPDH used as reference gene in RT-PCRs (f) Clustering of top 20 differentially regulated transcripts between WT and elm.

structural patterning and functional specification in apical gynoecium. Our *in-silico* analysis suggested that this gene is present as a single copy in chickpea and related legumes and has possibly acquired a broader function in regulating cell division and/or proliferation in multiple tissue types. Transcriptomics of *elm* and WT, highlighted possible role of gene 101503252 in cell division, mitotic cell cycle, cell wall metabolism, carbohydrate metabolism, cell wall organization, xyloglucan metabolic process and hemicellulose metabolic processes (Fig. 1f).

The present work identified a previously uncharacterized gene contributing to organ elongation and early vigor in chickpea that can be further explored to gain mechanistic insights into regulation of these traits and its exploitation in the breeding programs for increasing seed size and plant vigor.

Highlights of the work carried out by Golu Misra under the supervision of Dr. Archana Joshi-Saha (guide) as a part of his doctoral thesis work. This PhD thesis was submitted recently (Nov, 2024) to Homi Bhabha National Institute for the PhD Award in Life Sciences.

Genomic Basis of an Electron Beam Induced Mutant of Groundnut

Seed size plays an important role in groundnut (*Arachis hypogaea* L.) as it directly influences seed yield and market value. Being a quantitative trait, understanding the genetic basis of seed size is complex. However, usage of an induced mutant simplifies the approach of identifying the key genes governing seed size variation in groundnut. Towards this, we utilized an electron beam-induced large seed mutant, TG 89, to locate the genomic regions contributing to the seed size. This mutant has hundred kernel weight (HKW) of 75-82 g as compared to 40-48 g in its parent, TG 26. The histological analysis using Environmental Scanning Electron Microscopy (ESEM) revealed that the seed development in the mutant was primarily attributed to an increase in cotyledonary cell area rather than cell number. To map the genomic loci associated with the large seed size, a mapping population was developed by hybridization of TG 89 with normal seeded, genetically distant parent ICGV 15007 (Fig. 1A). A comprehensive genetic analysis of F_2 mapping population was carried out by utilizing simple sequence repeats (SSRs), miniature inverted-repeat transposable elements (MITEs), allele-specific and single nucleotide polymorphism (SNPs) markers. Initially, genotyping of the F_2 mapping population with 85 MITEs and SSRs revealed a significant QTL for seed size in the A05 linkage group, indicating potential regions for fine mapping. Towards fine mapping, 781 SNP markers were developed from genomic DNA sequencing using ddRAD-seq, of which 297 were utilized to construct a genetic linkage map spanning 20 linkage groups. QTL analysis identified two major QTLs on chromosomes A05 and A02, explaining notable phenotypic variance and two minor QTLs on B01 and B10 chromosomes (Fig. 1B). Interestingly, markers associated with the two major QTLs exhibited additive effects from either of the parental alleles, with the major positive additive effect contributed by the mutant allele in the '*mutant_qHKW_1*' (Fig. 1C). This primary QTL is originated from mutant and was mapped at 229 cM, spanning the genomic region 99.2–103.7 Mbp on the A05 chromosome (Fig. 1D). Markers flanking this mutant allele were developed and utilized to validate the QTL in other high yielding breeding lines. The analysis of candidate genes within this QTL region revealed various genes potentially involved in the regulation of seed size, including those coding for pentatricopeptide repeat (PPR) proteins, receptor kinase proteins, and notably, a gene, *arahy.5M7JWE*. Gene expression analysis with real-time PCR revealed a significant down-regulation of this gene *arahy.5M7JWE* in the mutant compared to the parent, suggesting that a recessive mutation in *arahy.5M7JWE* may be the cause of the observed phenotype in the mutant (Fig. 1E). This gene encodes the protein *Arahy.5M7JWE*, which belongs to the *Ah*TIFY family that is an ortholog of *BIG SEEDS1 (BS1)*, a plant-specific transcriptional repressor (Fig. 1F). This TIFY protein is known to play a crucial role in jasmonate signalling, a pathway well-known for its involvement in plant stress responses and seed and leaf developmental processes. The observed down regulation of *arahy.5M7JWE* in the mutant suggests the suppression of transcriptional repression by TIFY family proteins, thereby influencing seed size. These findings provide valuable insights into the genetic architecture of large seed trait in groundnut and offer potential target for future breeding efforts aimed at improving yield and quality characteristics.

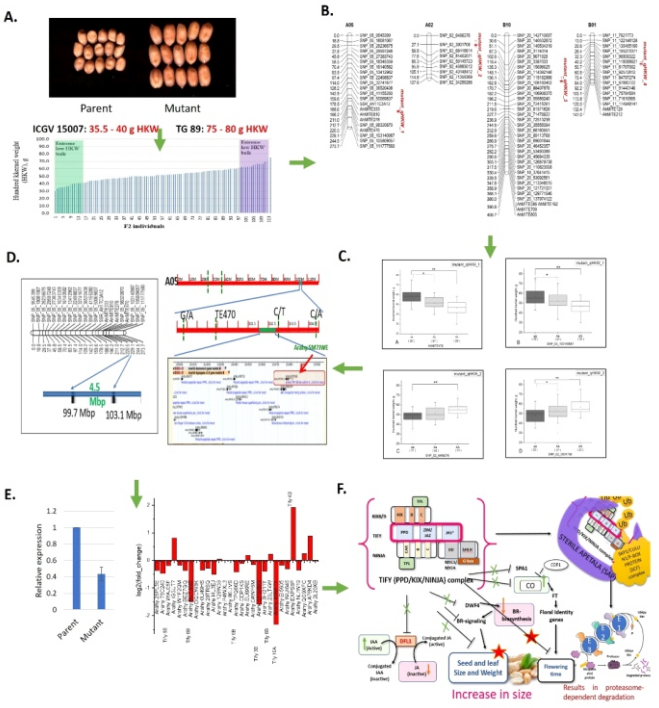

Fig.1: A). The variation in seed size of mutant TG 89, its parent TG 26, and F2 mapping population derived from the cross of ICGV 15007 and TG 89. B). QTLs detected for hundred kernel weight on the genetic linkage map. C). Allelic classification for hundred kernel weight for markers flanking two major QTLs. Solid line connecting box plots indicated additive effect while dotted line indicated dominance effect of allele D). Physical map corresponding to Mapped distance of mutant_HKW1. E). Relative expression of arahy.5M7JWE and other TIFY genes in mutant and parent. F). Schematic overview of the putative role of Tify protein in seed size control. The downregulation of the Tify protein, a transcriptional repressor, brings about the proteasome mediated degradation of the repressor complex, leading to alleviating the suppression of downstream pathways.

Highlights of the work carried out by Ms. Poonam Gajanan Bhad under the supervision of Dr. Anand M. Badigannavar, Professor, HBNI (Guide) and Dr. Suvendu Mondal (Technical Supervisor) as a part of her doctoral thesis work.

Molecular Mapping of Resistance Gene to Bacterial Leaf Pustule in Soybean

Soybean is the most important grain legume in the world in terms of production and international trade. It is an economically important leguminous crop for oil, feed, and soy food products. In India, soybean has become the number one oilseed crop and occupies the largest crop area in the rainfed *kharif* season. However, its continuous cultivation with a simultaneous increase in the area has led to increased incidences of several diseases, insects, and weeds. Among the various bacterial diseases, Bacterial Leaf Pustule (BLP), caused by *Xanthomonas axonopodis* pv. *glycines* (*Xag*), is a serious disease of soybean, particularly in northern and central India. The disease causes premature defoliation and consequent reduction in seed yield. The use of resistant cultivars is a cost effective and ecofriendly approach to minimize the losses due to disease. Progress in the development and use of BLP resistant soybean genotypes is hampered due to scarcity of high yielding BLP resistant soybean genotypes and further, unavailability of molecular markers linked to BLP resistance genes in Indian soybean genotypes. Keeping these points in view, the present study was taken up with major objectives including standardization of excised leaf technique and identification of resistance sources against BLP, molecular mapping of BLP resistance genes and their validation, biochemical changes in response to BLP and development of high yielding BLP resistance lies.

An excised leaf technique was standardized and 310 soybean lines were screened for BLP. The BLP resistant genotype (TS-3) identified in the study was used in hybridization with the BLP susceptible genotype (PK 472) and a segregating population was developed. Inheritance studies indicated that two recessive genes governed BLP resistance in soybean genotype TS-3.

Parental polymorphism followed by bulked segregant analysis identified 12 SSR markers, of which five SSR markers are located on chromosome 2 and seven SSR markers are located on chromosome 6, putatively linked to BLP resistance genes. Linkage analysis mapped the BLP resistance locus (*r1*) and five SSR markers (BARCSOYSSR_02_1585, BARCSOYSSR_02_1589, BARCSOYSSR_02_1590, BARCSOYSSR_02_1613 and Sat_183) on chromosome 2 with in a map distance of 5.5 cM (centiMorgon). Two SSR markers namely Sat_183 and BARCSOYSSR_02_1613 flank the r1 locus at a distance of 0.9 cM and 2.1 cM respectively. Similarly, second BLP resistance locus (*r2*) and seven SSR markers (BARCSOYSSR_06_0013, BARCSOYSSR_06_0024, BARCSOYSSR_06_0029, BARCSOYSSR_06_0040, Satt681, AW734043 and TSSR_06_01) were mapped on chromosome 6 (Fig.1). Two SSR markers BARCSOYSSR_06_0024 and BARCSOYSSR_06_0013 flank the *r2* locus at a distance of 1.5 cM and 2.1 cM respectively. All the flanking SSR markers identified in the study were validated on the 24 soybean genotypes, which included eight BLP resistant and fourteen BLP susceptible soybean genotypes along with the mapping parents. The SSR markers linked to resistance locus *r1* (Sat_183 and BARCSOYSSR_02_1613) and *r2* (BARCSOYSSR_06_0024 and BARCSOYSSR_06_0013) got amplified with the clear polymorphism that distinguishes the BLP resistant soybean genotypes from BLP susceptible genotypes. Biochemical studies indicated that the total phenolic and total flavonoid contents were higher in resistant genotype compared to the susceptible genotype. The total chlorophyll content was found to decrease rapidly in PK472 (susceptible genotype) compared to TS-3 (resistant genotype). Ten advanced selections, showing high yield potential and BLP resistance reaction, were identified. Among these, five resistant selections TSR-8, TSR-3, TSR-19, TSR-1 and TSR-7 gave significantly higher yield over the best check JS-335. The SSR markers tightly linked to BLP resistance loci identified in this study will help soybean breeders in marker assisted selection of BLP resistant sources.

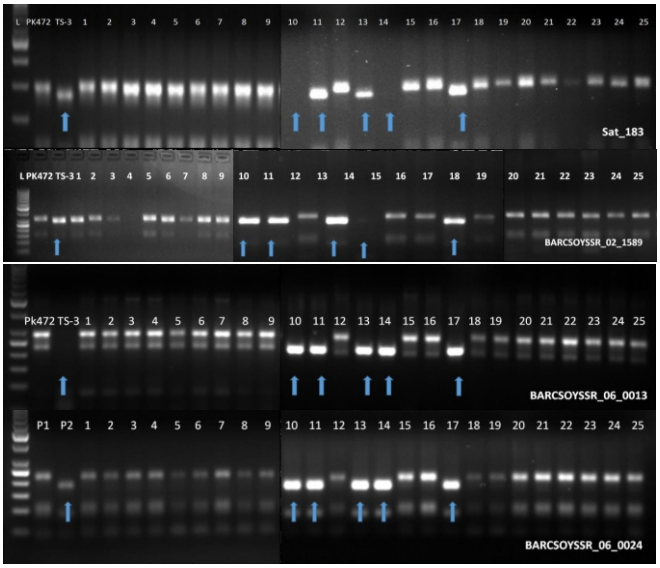

Fig.1: Genotyping of mapping population using SSR markers
Legend P1: PK472 (susceptible parent); P2: TS-3 (resistant parent); 1-25 F2 individuals; ⬆ Indicate resistant individuals.

Highlights of the work carried out by Sumit Prakashrao Totade under the supervision of Prof. J. G. Manjaya (Guide) and Dr. S. K. Gupta as a part of his doctoral thesis work. He was awarded PhD degree from Homi Bhabha National Institute in Life Sciences in 2023.

Radiation Induced Value Addition of Microalgae as Feed and Fuel

Microalgae are sunlight-driven factories that can turn fertilizer-rich water under sunlight into a vibrant green lawn within a day or two. They have received the most attention for their oil which can range from 50 to 60 % of their biomass. In the same area, the theoretical yield of oil from microalgae can be 10 times more than oil crop plants. Besides being bestowed with high photosynthetic rates, rapid growth, and ability to grow on wastelands, sewage water, and synthesize biomass rich in protein, carbohydrates, and oils, they can be further tuned to produce more oil by exposing to stress conditions (nutrient-limitation and high-salt condition) making them the 'Green gold' of the future. Microalgae-based bioproducts exploitation is limited to the production of fine chemicals such as carotenoids or as an aquaculture feed. The major bottleneck for utilizing microalgal oil in the fuel sector is the cost factor. The downstream applications such as harvesting and extraction contribute to increased expenses, while the use of PUFA from microalgae for food purposes is hindered by its low content. Nevertheless, starting with an oil-rich microalga can mitigate the above-listed drawbacks. Varying efforts have been made by researchers to produce oil-laden microalgae. In this view, we undertook the study to enhance oil production in microalgae using two different radiations (UV- and γ-rays).

The optimum dose for rapid oil accumulation along with minimum cell damage was finalized for both UV- (1 J/cm^2) and γ-radiation (1 kGy). Within 48 h, more than 1.5-fold increase in oil content was observed. Triacylglycerols were identified as one of the major constituents of accumulated oil. Radiation causes ionization of the molecules, and water constituting about 80 % of cytoplasm becomes the major target resulting in the formation of Reactive Oxygen Species (ROS). Apart from being highly reactive, ROS also serves as a secondary messenger for counteracting the cascade of damage. ROS was immediately measured after radiation and a more than 1.5-fold increase in ROS fluorescence was observed. To justify the role of ROS as a messenger towards enhancement in oil content, ROS formation was monitored under ascorbic acid (a physiological ROS scavenger) supplementation. UV- and γ-radiation-induced lipid accumulation was significantly reduced by 2.95-fold and 1.43-fold, respectively compared with their respective controls, indicating ROS as one of the major drivers of lipid accumulation. The molecular changes responsible for radiation-induced oil accumulation were also studied at different organizational levels using a systems biology-based approach. In brief, whole genome RNA-sequencing and SWATH-MS-based proteomics were used to identify the global reprogramming in genes and proteins, respectively. The integration of gene- and protein-level data as well as protein suggested the increase in abundance of starch-degrading enzymes, which implied the rerouting of carbon from starch towards oil accumulation. GC-MS-based fatty acid profiling revealed that UV-radiation favored the accumulation of saturated over unsaturated lipids; while γ-radiation treated lipids had a higher accumulation of an essential omega-3 fatty acid. Taken together, this study highlighted UV- and γ-radiation for inducing rapid lipid accumulation, which can impart value addition to microalgae-based "food-fuel" applications.

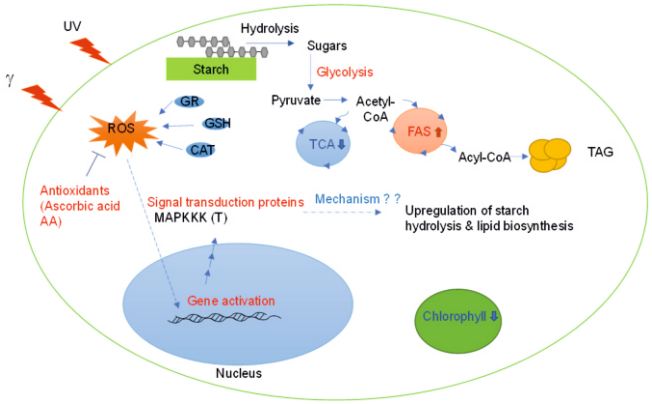

Fig.1: Radiation triggers "starch-to-oil" carbon-switching.
The pathways upregulated are indicated in red font while the downregulated in blue. Abbreviations: MAPKKK, mitogen-activated protein kinase kinase kinase; T, Transcript; TCA, tricarboxylic acid cycle; FAs, fatty acid biosynthesis; TAG, Triacylglycerol; GR, glutathione reductase; CAT, catalase; GSH, glutathione.

Highlights of the work caried out by Reema Devi Singh under the supervision of Dr. Ashish Kumar Srivastava (Guide) as a part of her doctoral thesis work. She was awarded a PhD. degree from Homi Bhabha National Institute in Life Sciences in 2023.

Salt Tolerance in Sugarcane: Lessons Learnt from a Radiation-induced Mutant

Sugarcane is a major food and biofuel crop of immense socio-economic relevance, on both national and global scale. Progressively increasing soil salinization in sugarcane-cultivating regions causes 25-30% reduction in cane yield and poor sugar recovery. This necessitates the development of robust and sustainable approaches for improving salt tolerance in sugarcane. However, due to its long life cycle and genome complexity, salt-adaptive mechanisms in sugarcane remain poorly understood. To address these lacunae, we characterized M4209, a promising salt-tolerant sugarcane mutant, derived from popular but salt-sensitive variety Co 86032, through radiation induced *in vitro* mutagenesis (RiMu).

Compared with Co 86032, M4209 exhibited 30% higher yield under saline field conditions, without significant yield penalties under control field conditions. This 'inducible salt tolerance' trait was investigated using a combination of transcriptomics and physio-biochemical studies. M4209 exhibited improved growth and survival under both moderate and severe salt stress, by maintaining ionic equilibrium, redox homeostasis, and photosynthetic efficiency. The activation of a chloroplast-centric transcriptional network in salt-stressed M4209 plants was suggestive of active nucleus-chloroplast communication. Thus, M4209's inducible salt tolerance was attributed to the salt-responsive transcriptional reprogramming of ion transport and antioxidant defense-related pathways, coupled with enhanced photosystem efficiency. Among the core genes associated with salt tolerance in M4209, a novel transcription factor, *SoSATA* (SALT-ACTIVATED TRANSCRIPTION ACTIVATOR), was selected for further characterization, due to its robust salt-responsive expression and putative regulatory function. The overexpression of *SoSATA* in Arabidopsis and soybean significantly improved plant growth under salt stress, suggesting its putative role as a positive regulator of salt tolerance.

At present, major sugarcane-cultivating states are facing the co-occurrence of increasing soil salinity with rising temperatures. However, the effect of combined heat and salt stress (HS-stress) and corresponding adaptive responses have not been investigated in sugarcane till date. Thus, a comparative evaluation of M4209 was performed under HS-stress scenario, wherein it exhibited significantly improved growth than Co 86032. In addition, M4209 exhibited lipid reprogramming towards higher plastidic:non-plastidic lipid ratio and lower root-to-shoot Na^+ translocation. Interestingly, M4209 exhibited a novel 'OSD' (Open Small Dense) stomatal phenotype, which was linked to an inherent transcriptional shift within the EPF9 (EPIDERMAL PATTERNING FACTOR 9)-EPF2 regulatory module. The OSD phenotype facilitated transpirational cooling and gas-exchange under HS-stress. This, coupled with enhanced photosynthetic assimilation, served as the major determinants of M4209's improved performance under HS-stress scenario. Our study demonstrates the enormous potential of the RiMu approach for development of agronomically important mutants in sugarcane, with the dual benefit of advancing fundamental understanding and accelerating crop-improvement programs.

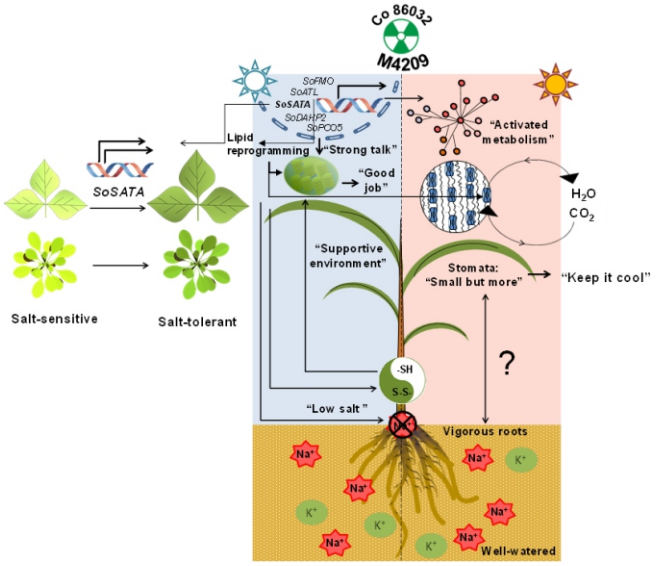

Fig.1: Proposed model for physio-molecular adaptions mediating improved tolerance to salt and HS stress in sugarcane mutant line M4209.

Highlights of the work carried out by Pooja Negi under the supervision of Dr. Ashish K. Srivastava (guide) as a part of her doctoral thesis work. She was awarded Ph.D. in Life Sciences from Homi Bhabha National Institute in 2024. [Best thesis award in SFRR-2024].

Functional Characterization of Site Specific Recombination System in *Deinococcus radiodurans*

During cell proliferation, the processes of DNA replication, genome segregation and cell division must be synchronized for stable inheritance of the genetic material. This is achieved by multiple checkpoint regulations in eukaryotes. But in prokaryotic cells, no such temporal or spatial regulatory mechanisms exist which would help in co-ordinating the various cellular processes together. Due to this reason, the eukaryotes are well suited to harbour multiple chromosomes whereas most bacterial cells harbour only a single chromosome in order to avoid any further complexity. But, the discovery of bacteria containing multiple chromosomes has raised attention-grabbing questions regarding the mechanisms involved in maintaining various genomic elements. One such bacterium is *Deinococcus radiodurans* which is an extremophile. It is one of the most radioresistant bacteria with a D_{10} value of 10 kGy i.e. about 3000 times the radiation tolerance of humans. It is a polyploid multipartite genome containing bacteria with two chromosomes and two plasmids which are tightly packed as compact doughnut shaped toroidal structure. The extreme phenotype of *D. radiodurans* can be attributed to its robust genomic structure, strong anti-oxidative stress response and an efficient DNA damage repair mechanism. But, how this unique genome architecture is maintained and segregated properly is still unknown. Bacteria in general contain circular chromosomes and chromosome dimers are formed after Bacteria in general contain circular chromosomes and chromosome dimers are formed after DNA replication. In *D. radiodurans*, the polyploidy increases the chances of formation of chromosome dimers. So, how these dimers are resolved and whether that has any significance to radiation resistance in this bacterium are the most intriguing questions.

The present study focuses on finding whether any chromosome dimer resolution system exists in *D. radiodurans* or not. The chromosome dimer resolution involves the function of site-specific recombination (SSR) system by tyrosine recombinases that could function independently or by the activation from the FtsK protein. Bioinformatics analysis has revealed that *D. radiodurans* encodes FtsK and six putative tyrosine recombinases. In-vivo functional role of FtsK in genome segregation and cell division is reported. For this, *ftsK-rfp* knock-in mutant cells expressing fluorescently tagged FtsK protein (FtsK-RFP) were generated. Time lapse imaging of live cells showed the dynamic movement of FtsK-RFP foci on the membrane and the nucleoid under normal conditions as well as post gamma irradiation (Fig. 1). Different domains of FtsK were also deleted from the genome which resulted in drastic changes in the nucleoid arrangement, cell membrane structure and cell morphology. Deletion of FtsK also resulted in delayed growth under normal (Unirr) and irradiated (Irr) conditions (Fig. 2A, B). All these results indicate towards an important role of FtsK in synchronizing the process of nucleoid separation with early cell division in *D. radiodurans*.

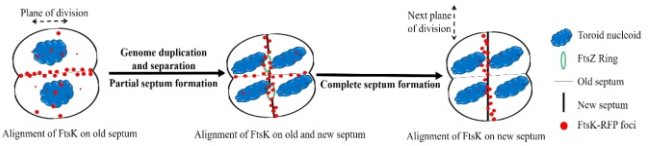

Fig.1: Schematic model of localization dynamics of FtsK during cell division in *Deinococcus radiodurans.*

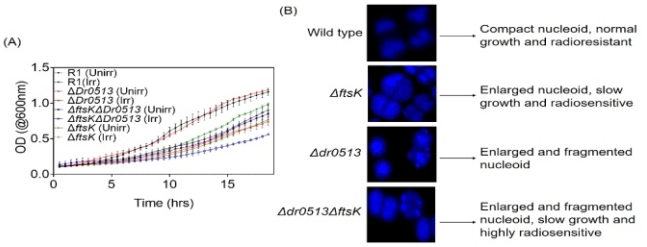

Fig.2: Deletion of FtsK and Dr0513 affects (A) the cell growth, the radioresistance and (B) the nucleoid structure in *Deinococcus radiodurans.*

The functional characterisation of one of the tyrosine recombinases of *D. radiodurans* (Dr0513) was also done. Deletion of coding sequence of Dr0513 leads to significant changes in the cells. In the absence of Dr0513, *D. radiodurans* cells failed to maintain the compact genome architecture. When both FtsK and Dr0513 were deleted from the cells, the growth was drastically reduced and various abnormal nucleoid arrangement was seen (Fig. 2A, B). Recombination assay showed that Dr0513 could perform SSR and FtsK could activate SSR.

All these results propose the functional significance of the site specific recombination system consisting of Dr0513 and DrFtsK in maintaining the unique nucleoid compactness of *D. radiodurans* R1. Lack of these proteins causes alterations in the nucleoid structure which ultimately effects the growth and gamma radiation response of the cells.

Highlights of the work carried out by Shruti Mishra under the supervision of Dr. Swathi Kota (Guide) as a part of her doctoral thesis work. This PhD thesis was submitted recently (Nov, 2024) to Homi Bhabha National Institute for the PhD Award in Life Sciences.